Component Analysis of Disaggregation of Pectin During Plate Module Ultrafiltration

P.D. HOAGLAND, G. KONJA, and M.L. FISHMAN

ABSTRACT

Concentration of commercial lime and citrus was carried out by plate module ultrafiltration with a 300K cut-off membrane with small changes in intrinsic viscosity and 48 and 55% recoveries. Subsequent ultrafiltration of permeates with a 100K cut-off membrane yielded pectins from retentates with lower viscosities and recoveries of 34 and 39%. Component analysis was applied to concentration and viscosity response curves from high performance size exclusion chromatography. Results suggested viscosity loss was due to passage through the membrane of small pectin molecules and/or aggregates released from breakdown of larger pectin aggregates during 300K ultrafiltration. Concentration of pectin with minimum loss of viscosity requires ultrafiltration which insures retention of small pectin aggregates. Improved component analysis was developed for characterizing solution behavior of pectin during processing.

Key Words: citrus, pectin, ultrafiltration, viscosity, aggregation

INTRODUCTION

THE ISOLATION and purification of pectin often involves large volumes of dilute aqueous solutions containing small molecules. Ultrafiltration can be applied to concentrate and purify them by removing from solutions of pectin both water ans small molecules. However, the behavior of pectin during ultrafiltration has not been extensively investigated and can be expected to be complex, due to formation of aggregates in sizes from ca. 100 kd to 10,000 kd (Fishman et al., 1992). Advances in component analysis of high performance size exclusion (HPSE) chromatographs of pectins from a variety of plants (Fishman et al., 1991a, b) allows study of the behavior of pectin during ultrafiltration in a highly aggregating system. Our objective was to apply an improved component analysis of HPSE chromatograms to determine whether pectin could be effectively concentrated by ultrafiltration. We also determined whether the viscosity of pectin could be improved by ultrafiltration through removal of low molecular weight pectins.

EXPERIMENTAL

High Performance size exclusion chromatography (HPSEC)

Waters μ-Bondagel E-High, E-1000, and SynChrom Synchropak GPC-100 columns were used in series. The mobile phase was 0.05*M* aqueous $NaNO_3$ (reagent grade) prepared with distilled water passed through a Modulab Polisher (Continental Water Systems Corp.) and filtered through a 0.2 μm Nucleopore. The solvent delivery system included a front-end Degasser ERC-3120 (Erma Optical Works, Ltd.) and a Beckman Model 110 Pump with a Model 421 Controller. The pump was fitted with two Waters M45 pulse dampeners and a Beckman pulse filter. A Beckman Model 210 injector valve with a 100 μL sample loop was positioned between the solvent delivery system and the column set maintained at 35° C in a thermostatted water bath. Nominal flow rate was 0.5 mL/min. Observed flow rate was determined with a horizontal 2 mL pipette connected to the RI Detector outlet. A ca. 0.1 mL bubble was injected into the exit stream and its passage through the pipette was accurately timed (Fishman et al., 1987). Flow rates were also obtained from the maximum peak position for material eluting at the total volume (V_s) of the system. This volume was determined from a series of sucrose injections (found to be 8.20 mL). Observed short term flow rate variation was <0.5%.

Authors Hoagland and Fishman are with the Eastern Regional Research Center, NAA, ARS, USDA, 600 East Mermaid Lane, Wyndmoor, PA 19118. Author Konja is with the University of Zagreb, Zagreb, Croatia.

Detectors

A differential refractive index RI Detector Model 7510, Erma Optical Works, Ltd., was used with a 30x preamplifier between its 1v integrator output and input to the A/D board. The detector was calibrated with dextran standards and gave a linear response from 0 to 8 mg/mL concentration of injected sample with a slope of 4843 ± 68 mv/mg/mL in the viscometer cell. A Differential Viscometer Model 100 (Viscotek Corp.) was operated at oven temperature 35° C. Periodically, inlet pressure was adjusted to 0 at zero flow to correct for drift (found related to overnight variations in room temperature). In addition to directly calculating specific viscosity from the differential pressure and inlet pressure (Fishman et al., 1989a), detector performance was evaluated with pullulan standards P-10, P-20, P-50, P-100, P-200, P-400, and P-800 from Polymer Laboratories. A plot of measured intrinsic viscosity (i.v.) vs. published i.v. for pullulans produced a straight line that passed through zero (Fig. 1). Specific viscosity, $\eta_{s.p}$ is defined by the relationship between excess pressure (DP) and inlet pressure. (P_o) by (1).

$$\eta_{s.p.} = \frac{4 \times DP}{(P_o - 2 \times DP)} \quad (1)$$

In dilute solution, we assumed that the intrinsic viscosity, i.v. ≅ $\eta_{s.p.}$ /c, where c is the concentration of solute. Moreover, as described by Fishman et al. (1989a), the area under the excess pressure (DP)

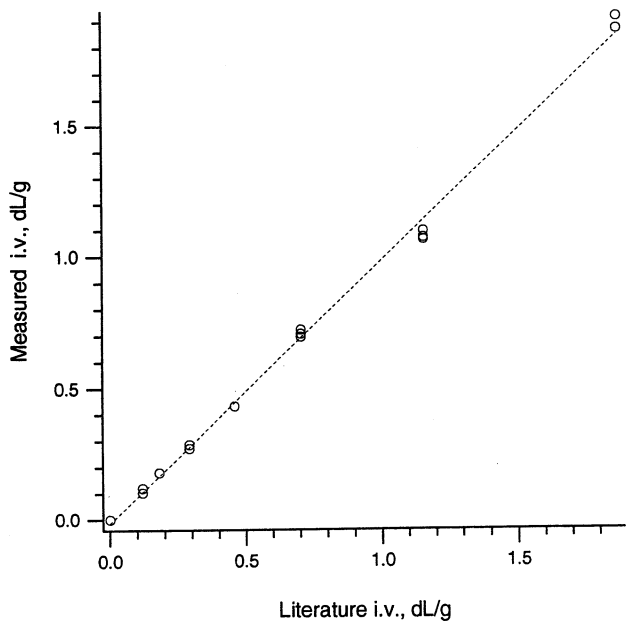

Fig. 1—Measured i.v. for pullulan standards (P-10, P-20, P-50, P-100, P-200, P-400, and P-800) compared to literature values (Fishman et al., 1987): Slope = 1.00 ± 0.01 with a correlation coefficient of 0.998.

Table 1—Weight average radius of gyration (R_{gw}) values for pullulan standards (Values obtained from equations for plots in Fig. 2)

Standard	MW_w[a]	[i.v.][a] dL/g	Polydispersity[a] Mz/Mw	R_{gz}[a] nm	R_{gw} nm
P-10	12,200	0.119	1.05	3.51	3.42
P-20	23,700	0.181	1.01	4.95	4.93
P-50	48,000	0.286	1.02	7.33	7.25
P-100	100,000	0.459	1.05	11.1	10.8
P-200	186,000	0.704	1.11	16.1	15.2
P-400	380,000	1.155	1.05	23.1	22.5
P-800	853,000	1.865	1.00	35.1	35.1

[a] Polymer Laboratories.

response curve gives the i.v. for the whole injected sample. The integrator output of each detector was input to a DT5712-PGL, Data Translation, A/D board installed in a IBM compatible PC. The digitized signals were processed with Unical 3.11 software from Viscotek. The Asyst *.DAT files from the Unical program were converted to ASCII text files in order to import raw data into other programs. P-800 and P-400, the two highest viscosity pullulans, produced a constant ratio of observed DP (excess pressure) response to RI (refractive index). These observations supported our assumption that the concentration of polysaccharide in the pressure transducer cell was low enough for the approximation i.v. $\cong \eta_{s.p.}/c$ to be valid. With fractionation of pectins in the columns, dilution of sample is greater than that for nearly monodisperse pullulans.

Sample preparation

Solutions of freeze-dried pectins (0.05%) were prepared with mobile phase and refrigerated. Each solution to be chromatographed was passed through a 0.45 μm filter before injection. The 100 μL sample loop was flushed with > 1 mL of solution to be chromatographed before injection. Samples were run in duplicate. The solutions tested were clear and showed no deterioration of properties during refrigerated storage for > 2 wk. Portions saved from original solutions of pectins used for ultrafiltration remained stable, as judged by HPSEC, for several days. Long term stability of freeze-dried pectins was verified by HPSEC.

Column calibration

Calibration of the system was carried out with the seven pullulan standards. Weight average molecular weights (MW_w), from light scattering, polydispersities (MW_z/MW_w), from equilibrium sedimentation, and i.v.'s were provided by Polymer Laboratories. Weight average radius of gyration (R_{gw}) values for these pullulans were obtained by curve fitting published values (Kato et al., 1982) for pullulan MW_w,R_{gz} (nm), and i.v. (dL/g) (Table 1) to (2), and (3), the Stokes-Einstein equation (Flory, 1953).

$$MW_w = A(R_{gw})^d \quad (2)$$

$$MW_w(\text{i.v.}) = B(R_{gw})^{3.000} \quad (3)$$

$$A = 1291 \qquad B = 35.76 \qquad d = 1.825$$

$$R_{gz} = R_{gw}([MW_z/MW_w]^{(1/d)}) \quad (4)$$

The fitted power law curves are shown in Fig. 2 and R_{gw} values are listed in Table 1. The elution volume, Ve, for each pullulan standard was determined by the peak maximum of the gaussian curve that fitted its concentration (RI) response curve. The sigma (half width at half height) for each gaussian curve varied with elution volume and, thereby, hydrodynamic volume. Sigma was consequently employed as an empirical measure of band spreading for each pullulan (see below). Void volumes (Vo) and total volumes (Vt = Vs − Vo) were measured according to Fishman et al. (1987). The distribution coefficient, K_{AV} was calculated from Ve with (5).

$$K_{AV} = (Ve - Vo)/Vt \quad (5)$$

Calibration curves for log(R_{gw}), size, and log(MW_w[i.v.]), a universal plot, were constructed (Fishman et al., 1987; 1989a) (Fig. 3).

Component analysis

We developed a general method to extract information from HPSE chromatograms by fitting gaussian components to concentration and

Table 2—% Weight and intrinsic viscosity (i.v.) of pectin recovered from ultrafiltrates[a]

	% Weight recovered	i.v., dL/g	% weight recovered × i.v.
Citrus pectin			
untreated		3.83	
300 kd retentate	55	4.25	2.34
100 kd retentate	39	1.51	0.59
permeate	7	n. m.	
total recovered i.v.			2.92
Lime pectin			
untreated		7.75	
300 kd retentate	48	7.52	3.61
100 kd retentate	34	3.41	1.16
permeate	19	n. m.	
total recovered i.v.			4.75

[a] All i.v.'s measured in 0.05*M* $NaNO_3$ at 35°C during HPSEC.
n. m. not measurable

viscosity response curves (Fishman et al., 1989b; 1991a, b). A gaussian component is characterized by peak elution volume, peak height, and sigma. The sigma, half-width at half-height of the gaussian component, is limited by band-spreading of the column set. The number of gaussian components required to fit a given response curve is determined by the total volume required by the curve and the sigmas assigned to the gaussian components. Peak elution volumes of neighboring gaussian components differ by about the sum of their sigmas. Two values for sigma have been applied to curve fitting (Fishman et al., 1991b). Sigma values of 0.274 mL for large R_g components of pectin and 0.11 mL for small R_g components were used in earlier work with different columns. We observed with the present columns, that response curves for pullulan standards could be fitted by one gaussian curve and the sigma derived therefrom had a distinct dependence on peak elution volume. In Fig. 4 is shown the power plot for gaussian sigma and pullulan K_{AV}. The linear best fit allows the sigma of each gaussian component to be related to the component elution volume during curve fitting. In the past, a concentration response curve was first fitted by a set of gaussian components. The component elution volumes were then fixed and the same component peak positions were applied to fitting the excess pressure response curve after adjustment for detector offset. Then, only component heights were allowed to vary to obtain a fit. We improved that approach by appending to the RI response curve the excess pressure response suitably offset by 4 to 5 mL to avoid overlap to place all experimental data points into one array. The Macintosh graphics program, Igor v1.24, (WaveMetrics, Lake Oswego, OR) enabled user defined curve fitting (up to 20 variables). The program implemented standard Gauss-Newton procedures for non-linear curve fitting (Press et al., 1988). We adapted the program to use up to 13 gaussian components to fit the combined concentration and viscosity response curve using Eq. (6). The elution time of a given viscosity gaussian component was set equal to the time for the corresponding concentration component plus its displacement corrected for detector offset (see Eq. 8). Thus up to seven variables representing elution times of concentration components and up to 13 or 14 variables representing heights of both concentration and viscosity components were used to fit Eq. (6) to the combined response curve. Initial estimates for variables were made to approximate a fit. The fitting procedure was well-behaved in every case, since the variables were constrained by two independent regions of the combined response curve.

fitted response area =

$$\sum_{t=8}^{17}\left[\sum_{i=1}^{7} RI_{it} + \sum_{j=1}^{6} DP_{j(t+\text{displace})}\right] \quad (6)$$

$$RI_{it} = \sum_{t=8}^{17} (h_{RIi})e^{-[T_{RIi}-t)^2/2\sigma_i^2]} \quad (7)$$

$$DP_{j(t+\text{displace})} = \sum_{t=8}^{17} (h_{RIi})e^{-[(T_{RIi}+\text{displace}-t)^2/2\sigma_i^2]} \quad (8)$$

$$\text{Displace (min)} = (5 - 0.1074)(\text{mL})/[\text{FR(min/mL)}] \quad (9)$$

RI_{it} was the combined RI response for each component and $DP_{j(t+displace)}$ was the combined excess pressure response for each component. T_{RIi}, and h_{RIi}, were gaussian concentration component i elution time and height at peak maximum and h_{P_j} was viscosity component peak height. FR was the flowrate. Component sigma (σ) was related

Table 3—Properties of HPSEC components of citrus and lime pectins

Pectin	Components 1	2	3	4	5	6	7	8	9	wt avg
				R_g, nm × 10 (Å)						
Citrus untreated			410	221	133	86	58	40	30	208
Citrus 300 kd retentate			411	231	144	95	62	40	30	220
Citrus 100 kd retentate			372	197	130	90	61	42	27	113
Citrus 100 kd permeate					141	96	70	53	40	86
Lime untreated	1157	673	380	219	151	90	55			599
Lime 300 kd retentate		592	346	196	121	79	52	36		297
Lime 100 kd retentate			354	201	124	81	54	36		181
				Weight fraction						
Citrus untreated			0.224	0.301	0.248	0.145	0.060	0.016	0.007	
Citrus 300 kd retentate			0.231	0.310	0.251	0.148	0.051	0.009	0.000	
Citrus 100 kd retentate			0.029	0.120	0.273	0.331	0.179	0.051	0.017	
Citrus 100 kd permeate					0.166	0.340	0.272	0.175	0.046	
Lime untreated	0.233	0.278	0.291	0.086	0.065	0.029	0.019			
Lime 300 kd retentate		0.159	0.393	0.229	0.136	0.060	0.018	0.005		
Lime 100 kd retentate			0.209	0.286	0.266	0.158	0.063	0.018		
				i.v., dL/g						
Citrus untreated			8.35	4.00	2.00	1.20	0.60			3.78
Citrus 300 kd retentate			8.92	4.34	2.35	1.24	0.60			4.21
Citrus 100 kd retentate			8.26	3.81	1.76	0.73	0.40			1.49
Lime untreated	14.44	9.95	4.70	2.50	1.68	1.10				7.85
Lime 300 kd retentate		17.63	8.76	3.73	1.80	0.89				7.40
Lime 100 kd retentate			8.20	3.58	1.84	0.50				3.31

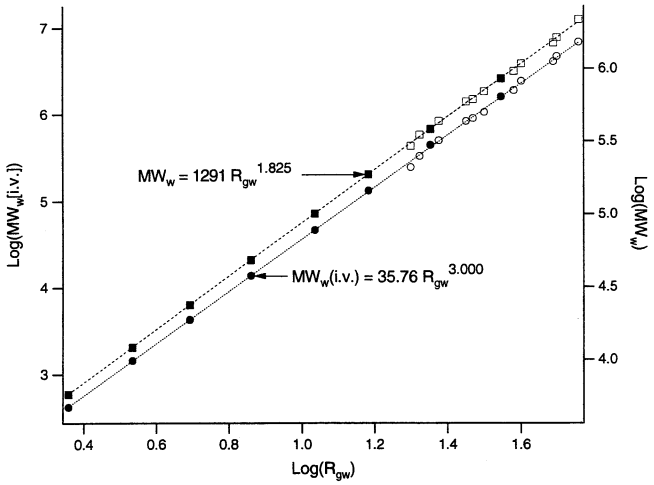

Fig. 2—Fitted curves of log(MW_w) and log(MW_w[i.v.]) to log(R_{gw}) for pullulan standards. Open circles and squares are pullulan values from Kato et al. (1982). Filled circles and squares are logs of pullulan values in Table 1 and P-5.

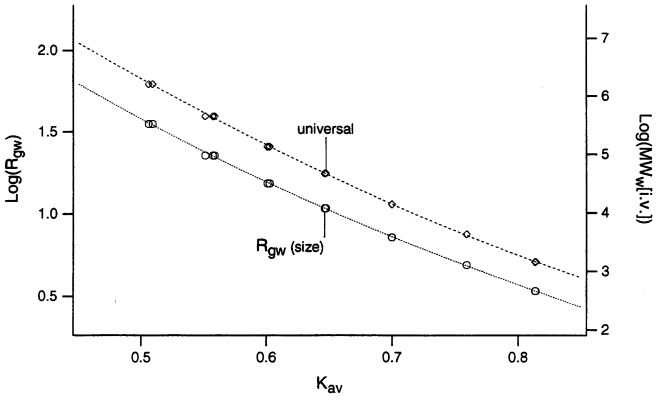

Fig. 3—Size (R_{gw}) and universal (MW_w[i.v.]) calibration curves for column set based on distribution coefficients (K_{AV}) for pullulan standards.

to T_{RI_i} component elution time with (10) obtained from the linear best fit (Fig. 4) with the following assumptions:

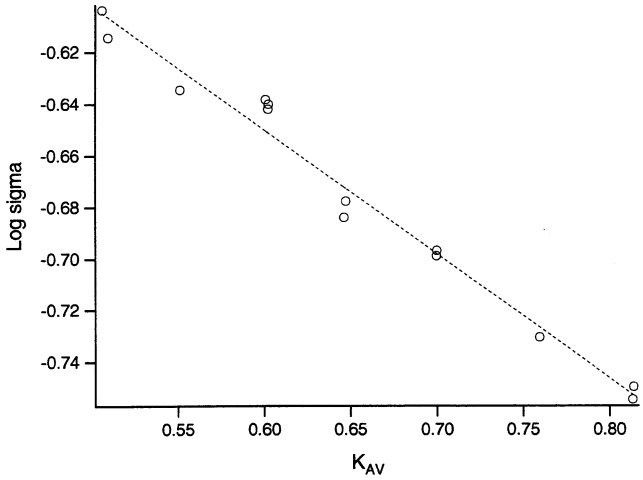

Fig. 4—Sigmas for gaussian curve fitted to pullulan RI response curves plotted as a function of K_{AV}. Linear fit used for equation (9).

1. Maximum σ = 0.25 mL
2. Minimum σ = 0.12 mL

$$\log(\sigma) = -0.602 - 0.106\, T_{RI_i} \times FR - \log(FR) \qquad (10)$$

Global weight average i.v. was calculated as the sum of the products of component weight fraction and component i.v. A fitted i.v. response curve was calculated for each point of the fitted concentration response curve with (11). This curve was then compared to the observed i.v. response curve. The

$$IV_{fitted} = \sum_{i=1}^{6} \frac{IV_i \times (h_{RI_i}) e^{-[(TRI_i - t)^2/2\sigma_i^2]}}{\sum_{i=1}^{6} (h_{RI_i}) e^{-[(TRI_i - t)^2/2\sigma_i^2]}} \qquad (11)$$

observed i.v. response curve was calculated from the ratio of each point of the observed excess pressure curve, baseline and detector offset corrected, to the point of the observed concentration response curve, baseline corrected. A fitted R_{gw} response curve was calculated from component R_{gw}'s with Eq. (12).

$$R_{g\ fitted} = \sum_{i=1}^{7} \frac{R_{gi} \times (h_{RI_i}) e^{-[(TRI_i - t)^2/2\sigma_i^2]}}{\sum_{i=1}^{7} (h_{RI_i}) e^{-[(TRI_i - t)^2/2\sigma_i^2]}} \qquad (12)$$

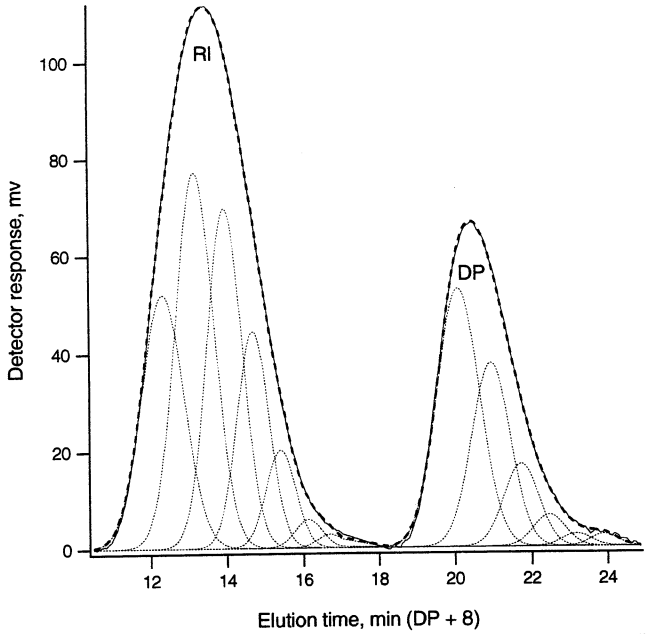

Fig. 5—11 Gaussian curves fitted to combined concentration (RI) and viscosity (excess pressure, DP) response curve for untreated citrus pectin. Components are numbered from left to right in decreasing size.

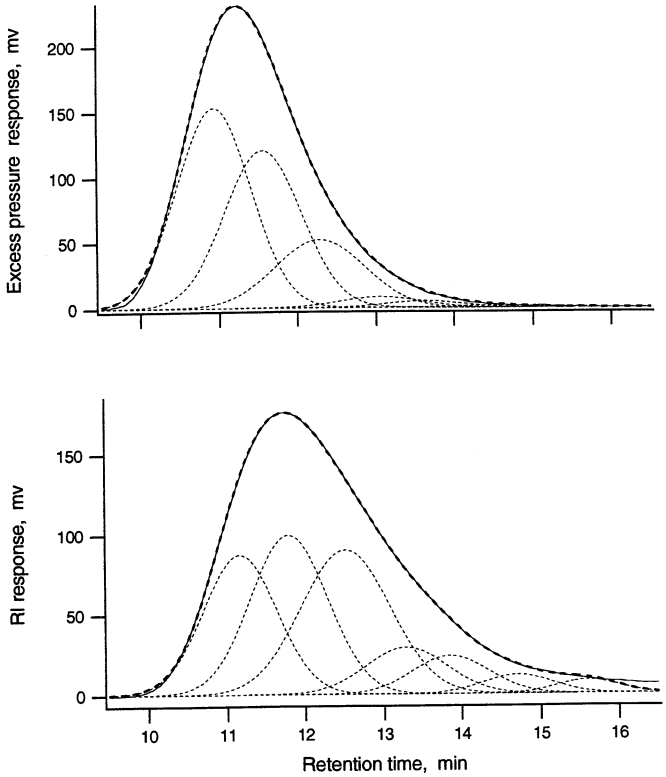

Fig. 6—HPSE chromatogram of untreated lime pectin with concentration (RI) and viscosity (excess pressure) detection (solid line). Analysis gave seven concentration components with five matching viscosity components (light dashed lines). Heavy dashed line is the fitted total response of all the respective components.

Plate module ultrafiltration

A laboratory size Minitan Ultrafiltration System, XX42MT060, Millipore Corporation, fitted with four plates, was used at room temperature (≈ 23°C). The system was cleaned and sterilized following recommended procedures. The sanitary stainless steel cell was fitted with four PTHK Minitan plates, 300K or 100K NMWL, part no. PTMK OMP 04. Pectin (6.0g) was dissolved in 1200 mL 0.05 *M* $NaNO_3$. A 50 mL portion of the starting solution was set aside. Solutions were ultrafiltered at flux rate 35 mL/min, starting temperature 17°C with initial back pressure 0.5 bar. Filtration was stopped at 1.2 bar (temperature was 26°C). The 300K retentate for lime pectin was 370 mL and for citrus pectin was 320 mL. A 50 mL portion of 300K permeate was set aside. The remaining 300K permeate was then ultrafiltered through a 100K membrane, using the same starting and ending back pressures. All solutions were then dialyzed vs. water at 4°C and pectins were recovered by freeze-drying. All ultrafiltrations were completed within 2 hr. Overall 4 fold concentration was obtained.

Pectins

The lime pectin, SRS-1500, 73.9% degree methoxylation I.F.T. sag 231 was obtained from Grinsted Products, Inc. (Industrial Airport, KS). The citrus pectin (largely from lemon) was a rapid set, type 104, 70% degree of methoxylation from Bulmers, Limited (Hereford, England).

RESULTS

Plate module ultrafiltration

With citrus pectin, 55% of starting material was recovered from the 300K retentate (Table 2) and had an i.v. of 4.25 dL/g. The pectin recovered from the 100K retentate, which had passed through the 300K membrane, (i.v. 1.51 dL/g) was 39% of the starting material. A net decrease of viscosity occurred as evidenced by total recovered i.v. of (0.55 × 4.23 + 0.39 × 1.51) = 2.92 dL/g. Loss of nearly 50% of the original citrus pectin by ultrafiltration through the 300K membrane resulted in a 10% improvement is viscosity. The lime pectin (i.v. 7.75 dL/g) was about twice the value for citrus pectin. Though only 48% of lime pectin was recovered from ultrafiltration through the 300K membrane, the i.v. of retentate was less (7.52 dL/g). No increase in viscosity was obtained; 34% of original lime pectin was recovered from the 100K retentate. The 100K permeate contained 19% of lime pectin that had passed through both membranes.

Component analysis

The areas under response curves for citrus and lime pectins were fitted by nine components. One example fit for a combined response curve for citrus pectin is shown (Fig. 5). The combined fit was used to construct a final fit. One representative final fit for lime pectin is shown (Fig. 6). Values for component R_{gw} weight fraction and i.v. are presented (Table 3). An estimate of precision was made from these results and analyses of polysaccharide gums (Hoagland et al., 1993). Usually most of the weight fraction was accounted for by the first two components, with the following reproducibility errors: component 1 R_{gw} <2%, i.v. <3%; component 2 R_{gw} <4%, i.v. <6%. Other components had larger errors associated with low weight fraction values and typically ranged for R_{gw} from 5–10% and for i.v. from 7–15%. Whenever low signal-to-noise ratios were encountered with the excess pressure response i.v.'s were not calculated.

Citrus pectin did not have components 1 and 2 (Table 3) which were found for lime pectin. 300K retentate citrus pectin had components 3, 4, and 5 of greater weight fractions than corresponding components of original pectin. These three components also had i.v.'s greater than those corresponding from untreated citrus pectin. This accounts for the greater i.v. of 300K retentate citrus pectin. Compared to 300K retentate citrus pectin, that recovered from 100K retentate had marked reduction in weight fraction values for components 3 and 4, which accounts for the notably reduced i.v. (1.51 dL/g) of that fraction. Citrus pectin from the 100K membrane permeate showed no components 3 and 4 and was rich in components 6 and 7.

In general, corresponding components from all citrus pectin fractions had similar values for R_{gw}, and i.v. Lime pectin did not exhibit values for R_{gw}, and i.v. for components 1–5 that corresponded to untreated and 300K retentate material. Components for 300K retentate were similar to those of 100K retentate lime pectin. Lime pectin permeate eluted almost entirely in the total (small size) volume of the column set and could not be analyzed. Component 1 of untreated lime pectin was unusually large and had a large i.v. (14.4 dL/g). Although this component was not found in 300K retentate lime pectin, a high viscosity component 2 was found in that fraction. Large-sized-component 1 lime pectin (weight fraction 0.233) upon ultrafiltration was converted to smaller-sized-component 2 material (weight fraction 0.159) with greater viscosity.

Observed i.v.

In all cases close correspondence was found between observed i.v., calculated from the point-by-point ratio of excess pressure response to concentration (RI) response, and fitted i.v.'s from component analysis (Fig. 7). The global weight average i.v.'s (Table 3) agreed well with measured i.v. values. A weight average R_{gw} for each pectin was also obtained from component analysis. Plots of log(fitted i.v.) vs. log(fitted R_{gw}) were developed (Fig. 8) for both citrus and lime pectins. The plots for citrus pectin were linear over the first ~ 80% of the response curves and passed through values calculated for individual components. Slopes were similar (~1.20). The plot for untreated lime pectin was non-linear and did not pass exactly through component values. Linearity over the first 80% of total elution time was observed for both 300K and 100K retentate lime pectins. Slopes were: 300K retentate lime pectin, 1.45 and 100K retentate pectin, 1.37.

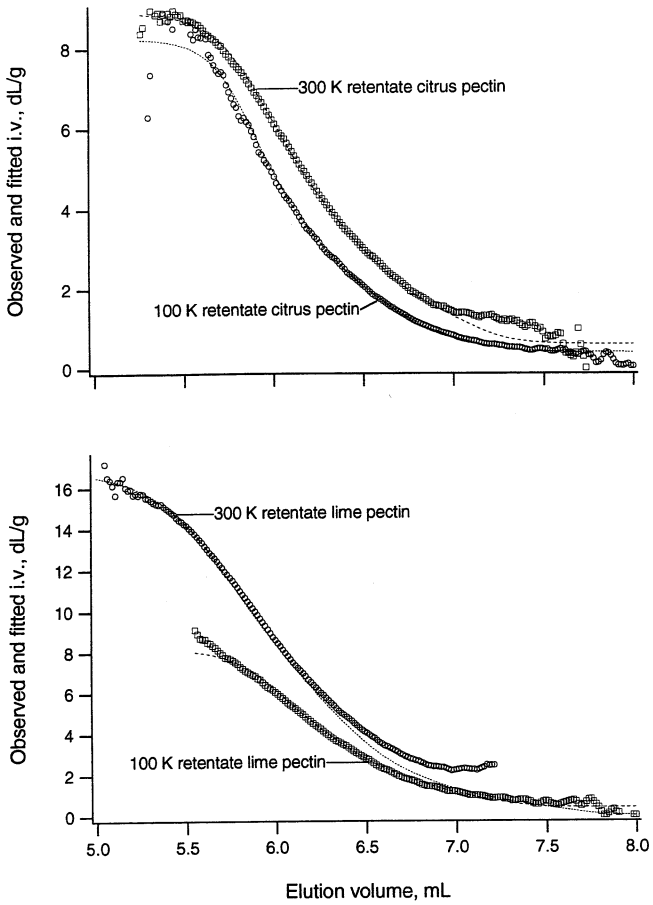

Fig. 7—Fitted i.v. response curves and measured i.v. for citrus pectin (top) from 300K retentate and 100K retentate, and for lime pectin (bottom) from 300K retentate and 100K retentate. Dashed lines are fitted responses.

DISCUSSION

Citrus pectin

The results from plate module ultrafiltration of citrus pectin demonstrate improvements in i.v. were achieved with 300K membrane ultrafiltration. However, material loss was substantial and there was net loss of i.v. as based on total recovered i.v. of the 100K retentate pectin. This loss could be explained by the capacity of pectin to form stable aggregates in solution. Apparently, during ultrafiltration, as documented by changes in weight fractions for citrus pectin components (Table 3), pectin fragments (i.e., sub-aggregates or molecules) migrated from components 3 and 4, and either passed through the 300K membrane or became part of components 5–9. Much of the smaller-sized pectin that passed through the 300K membrane was retained by the 100K membrane. The size distribution of that fraction, however, was notably shifted towards the lower end (Table 3, weight averages, citrus pectin 100K retentate). This shift could be a consequence of enrichment of the fraction with low molecular weight pectin oligomers and/or neutral sugar side chain fragments that may compete with larger pectin molecules for aggregation sites. These aggregates can be very stable. Mort et al. (1991) have shown that pectin oligomers were retained after dialysis of pectin vs. water for several days, and chelating agents such as CDTA were incompletely removed by dialysis. Fishman et al. (1989b) observed that low molecular weight aggregates or molecules of tomato pectin did not dialyze vs. water, but passed through the membrane during dialysis vs 0.05*M* NaCl. In earlier work with citrus pectin Fishman et al. (1984) also showed low molecular weight material recovered from dialysate could form large aggregates in water. An aggregation site is usually considered a "junction zone" (Rees, 1982), an intermolecular union between homologous galacturonan regions of pectin molecules. Galacturonan regions are demarcated by an α-(1-2) rhamnose residue which introduces an abrupt redirection of the adjoining galacturonan region. This redirection has been labeled a "kink" by Rees and Wight (1971). The overall shape of a large pectin molecule with one or more rhamnose residues is that of a segmented rod, since the galacturonan regions are relatively stiff and straight. Junction zones can be stabilized by multiple hydrogen bonds between ~25 or more galacturonate residues, or by Ca^{+2} salt bridges between galacturonate carboxylate groups (co-operative sequential binding, Kohn, 1975). Probably hydrophobic interactions between methyl groups also stabilize them in those instances where the galacturonan region is block methyl esterified (Oakenfull and Scott, 1984). Some junction zones may be stabilized by interactions between neutral sugar side chains that are sometimes attached to rhamnose residues (1-4 linkage) and are believed to be concentrated in "hairy regions" of some pectin molecules. Possibly, the larger citrus pectin molecules recovered from 100K retentate have a notable proportion of junction zones involved with pectin oligomers and a reduced proportion of end-to-end junction zones. This latter type junction zone would lead to formation of larger aggregates. We suspect that large pectin aggregates may consist of long end-to-end junction zone-joined segmented rods stabilized by interchain bridges made by shorter length pectin molecules. Gel networking would require at least three possible junction zone sites and chaining of pectin molecules would require at least two similar sites. These conditions apparently prevailed in structures for pectin aggregates recently visualized by transmitting electron microscopy (Fishman et al., 1992). Seen were long rod-like units joined to apparent segment-segment kink points. It is not possible now to estimate the extent of segment-segment overlap between 2 pectin molecules that form a junction zone. Many junction zones seen for pectin gel particles break up in high ionic strength solution (Fishman et al., 1992).

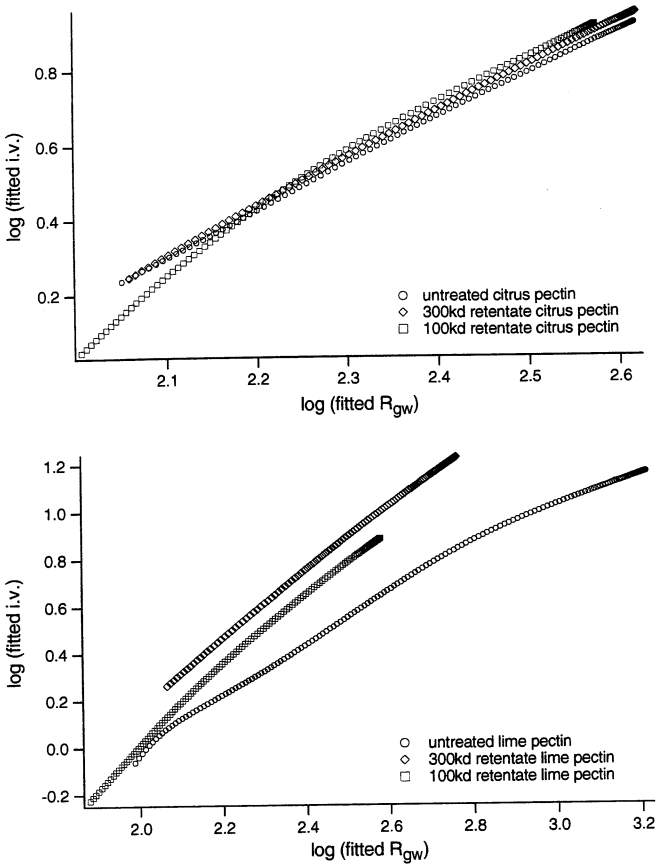

Fig. 8—Log-log plots of fitted i.v. against fitted R_{gw} for citrus pectins (top) and lime pectins (bottom).

Apparently, from microgel micrographs segmented rods of pectin organized into spherical macro-assemblies about 1000 nm in diameter. The mobile phase for HPSEC was chosen to be 0.05*M* $NaNO_3$ so that enough junction zones would be broken to produce sizes of pectin aggregates within the fractionating range of the column set (ca. R_{gw}, 2 to ~100 nm). When water was the mobile phase for HPSEC, pectins eluted near the void volume (Fishman et al., 1989a).

Nonoverlapping binding of pectin oligomers to pectin molecules with at least two segments could be expected to have a profound effect on the i.v. of the aggregate. Compared to the original pectin molecule, the MW of the aggregate would increase whereas the length and R_g, of the aggregate would be mostly unchanged. As pointed out earlier (Fishman et al., 1991b) given the Stokes-Einstein relationship (13), (Flory, 1953),

$$\text{MW(i.v.)} = AR_g^3 \qquad (13)$$

at constant R_g, i.v. could be expected to decrease in response to any increase in aggregate MW due to nonoverlapping binding between large pectin molecules and pectin oligomers (DP < 25, for example, see Fishman et al., 1991b). Nonoverlapping bundling of oligomers to larger pectin molecules with measurable i.v. may have contributed to overall loss of viscosity for citrus pectin during ultrafiltration.

Lime pectin

The lime pectin was distinguished from citrus pectin by its greater i.v. and by component 1 and component 2 material by HPSEC. No other pectin has been found to correspond to component 1 in our analysis. Because untreated lime pectin was analyzed directly, without dialysis or centrifugation, we believe component 1 represented microgel particles. These could be similar to gel particles visualized by TEM (Fishman et al., 1992) and often encountered in light scattering investigations (Jordan and Brandt, 1978, Chapman et al., 1987; Berth, 1988). During ultrafiltration such gel particles were possibly opened by shearing induced by turbulent flow in the apparatus. They then appeared as large aggregates in component 2 material from lime pectin in 300K retentate (Table 3). Since gel particles are nondraining, they should exhibit lower i.v. than a more extended aggregate of about the same size. Component 2 lime pectin from the 300K retentate may represent aggregates about half the size of component 1 microgel particles with greater viscosity resulting from a less symmetrical and perhaps more freely-draining structure. The good correspondence between fitted i.v. and observed i.v. (Fig. 7) indicates that observed i.v. at any time could be expressed as combined i.v.'s of those components with measurable viscosity. Any given data point of a concentration response curve could be viewed as the summation of the contribution of each component to both fitted i.v. and R_{gw}. The contribution of a given component is the weight average of that component in the given data point. We therefore constructed power plots for fitted values of i.v. and R_{gw} (Fig. 8). A change in shape of macromolecular assemblies of lime pectin is suggested by distinct downward curvature at the large size end. This curvature indicates a reduction of $d\log(\text{i.v.})/d\log(R_{gw})$, with increasing size. This may reflect the contribution to observed i.v. by larger sized, lower i.v. microgel particles. Anger and Berth (1985, 1986) and Berth (1988) reported a similar downward curvature for sunflower and citrus pectins for Mark-Houwink power plots of log(i.v.) vs log(MW_w). They presented strong evidence for microgel particles with lower i.v. than would be expected for single, extended large ($>10^6$ MW) pectin chains.

Similar plots for the citrus pectins (Fig. 8) show a common slope of ca. 1.20 for large sized pectin aggregates. This indicated that a common geometry was probably shared between component 3–5 citrus pectin aggregates. Anger and Berth (1986) found a Mark-Houwink exponent (α) of 0.73 for citrus pectin:

$$\text{i.v.} = (9.55 \times 10^{-4})MW_w^{0.73}. \qquad (14)$$

For a MW_w of 100,000 an i.v. of 4.27 dL/g was calculated. These values were close to the i.v. value 4.34 dL/g for component 4 of 300K retentate citrus pectin (Table 3) and the value for MW_w of 107,000 (Table 4). A Mark-Houwink α of 0.746 was obtained from a power plot for components 3–5, which represent about 80% of the weight fraction of the eluted citrus pectin.

$$\text{i.v.} = (7.67 \times 10^{-4})MW_w^{0.75} \qquad (15)$$

The agreement between (14) and (15) is good, but can be tempered with the following considerations: if citrus pectin is aggregating then scaling laws would best apply if (1) aggregates were self-similar in shape (i.e. fractal) and (2) concentration of pectin monomers was negligible. The similarity of pectin aggregate shape may be evaluated by linearity of log(fitted i.v.) vs. log(fitted R_{gw}) plots. For HPSEC with viscosity-concentration detection, a power i.v. ~R_{gw} plot may be more precise than the Mark-Houwink plot since, in this latter instance, MW_w must be calculated indirectly from a universal log(MW_w[i.v.]) calibration curve. Berth (1988), Brigand et al. (1990), and Kravtchenko et al. (1992) have shown that the chemical composition of industrial pectins was not uniform throughout the elution volume during size exclusion chromatography. Therefore, any interpretation of power law plots, such as log(i.v.) vs log(R_{gw}) should take into consideration molecular inhomogeneity, aggregation size inhomogeneity, and shape changes resulting from microgel particle formation. For example, the power law plots for components for 300K retentate citrus pectin and 100K retentate lime pectin (Fig. 9) gave distinctly different slopes for log(MW_w) vs log(R_{gw}). The slope of 1.36 for lime pectin indicates more extended, relatively inflexible conformations than citrus pectin

Table 4—MWw of components of citrus and lime pectins from universal calibration (Fig. 3)

Pectin	Components						
	1	2	3	4	5	6	7
Citrus untreated			302,000	102,000	43,500	19,000	11,300
Citrus 300 kd retentate			285,000	107,000	47,700	24,700	14,200
Citrus 100 kd retentate			231,000	75,900	46,600	36,500	20,400
Lime untreated	3,260,000	1,053,000	433,000	159,000	76,600	24,100	
Lime 300 kd retentate		413,000	176,500	76,300	36,200	19,600	12,500
Lime 100 kd retentate			200,000	85,800	38,100	22,300	11,100

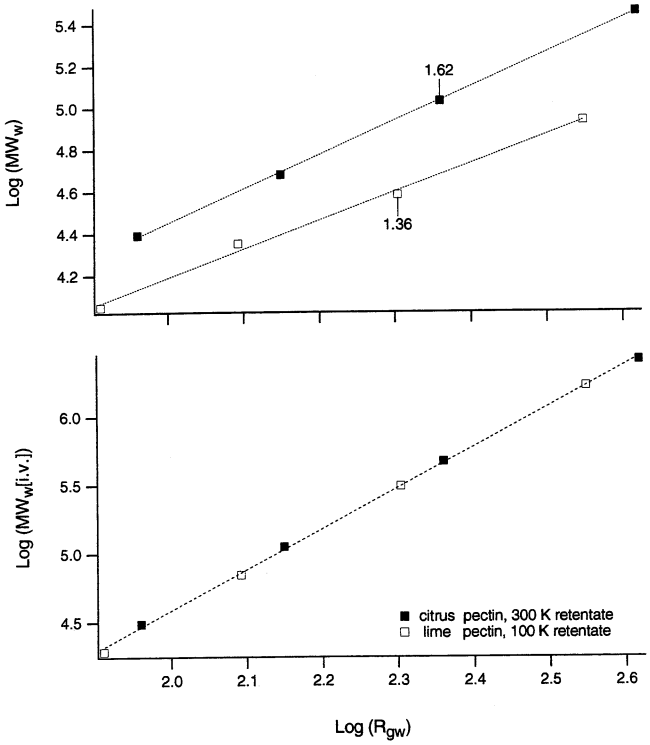

Fig. 9—Log-log plots for MW_w[i.v.], i.v., and MW_w vs R_{gw} for components from 100K retentate lime pectin and 300K retentate citrus pectin. Einstein (MW_w[i.v.]) plot has expected slope of 3.0. Indicated slopes for MW_w are significantly different and suggests a difference in shapes and/or aggregation.

(slope = 1.62). This points to the possibility that citrus pectin aggregates have significantly different shapes than lime pectin aggregates.

Component analysis

This method has been applied to characterization of pectins from many sources (Fishman et al., 1991a), to changes in pectin during fruit maturation (Fishman et al., 1991b), and to polysaccharide gums (Hoagland et al., 1993). We have now demonstrated that it can be applied to monitoring changes in viscosity during processing of pectin in laboratory or, presumably, in larger-scaled operations. In the past most pectins were characterized by 4–5 components with similar sigmas, 0.274 mL (Fishman et al., 1991b). With more highly resolving columns and by determining sigmas for pullulan standards we have improved the method for analysis to include up to 7 components. Precision of the fitting procedure has also been improved by simultaneously, rather than sequentially, fitting both viscosity and concentration response curves. Component analysis can be applied to draw fine distinctions between variable pectin preparations in terms of viscosity and molecular size, and their distributions under tightly controlled conditions for chromatography. Such information may be obtained from a limited number of samples without requiring fractionation. Meaningful results from component analysis, of course, directly rely on accurate column calibration.

CONCLUSIONS

HPSEC and component analysis can be used to monitor ultrafiltration of pectin to reveal changes in distributions of aggregate size and intrinsic viscosities. The chemical diversity of pectin, along with its propensity to aggregate, are complicating factors for determining acceptable conditions for ultrafiltration. Loss of aggregate-stabilizing-small pectin molecules must be avoided by using small pore size membranes (such as 100K) for ultrafiltration. Apparently, even when loss of low molecular weight material is prevented, little improvement in pectin viscosity may be expected. Under favorable conditions ultrafiltration could be applied to concentrate pectin.

REFERENCES

Anger, H. and Berth, G. 1985. Gel permeation chromatography of sunflower pectin. Carbohydr. Polym. 5: 241–250.
Anger, H. and Berth, G. 1986. Gel permeation chromatography and the Mark-Houwink relation for pectins with different degrees of esterification. Carbohydr. Polym. 6: 193–202.
Berth, G. 1988. Studies on the heterogeneity of citrus pectin by gel permeation chromatography on Sepharose 2 B/Sepharose 4 B. Carbohydr. Polym. 8: 105–117.
Brigand, G., Denis, A., Grall, M., and Lecacheux, D. 1990. Insight into the structure of pectin by high performance chromatographic methods. Carbohydr. Polym. 12: 61–77.
Chapman, H.D., Morris, V.J., Selvendran, R.R., and O'Neill, M.A. 1987. Static and dynamic light-scattering studies of pectic polysaccharides from the middle lamellae and primary cell wall of cider apples. Carbohydr. Res. 165: 53–68.
Fishman, M.L., Cooke, P., Levaj, B., Gillespie, D.T., Sondey, S.M., and Scorza, R. 1992. Pectin microgels and their subunit structure. Arch. Biochem. Biophys. 294: 253–260.
Fishman, M.L., Damert, W.C., Phillips, J.G., and Barford, R.A. 1987. Evaluation of root mean square radius of gyration as a parameter for universal calibration of polysaccharides. Carbohydr. Res. 160: 215–225.
Fishman, M.L., El-Atawy, Y.S., Sondey, S.M., Gillespie, D.T., and Hicks, K.B. 1991a. Component and global average radii of gyration of pectins from various sources. Carbohydr. Polym. 15: 89–104.
Fishman, M.L., Gillespie, D.T., Sondey, S.M., and Barford, R.A. 1989a. Characterization of pectins by size exclusion chromatography in conjunction with viscosity detection. J. Agric. Food Chem. 37: 584–591.
Fishman, M.L., Gillespie, D.T., Sondey, S.M., and El-Atawy, Y.S. 1991b. Intrinsic viscosity and molecular weight of pectin components. Carbohydr. Res. 215: 91–104.
Fishman, M.L., Gross, K.C., Gillespie, D.T., and Sondey, S.M. 1989b. Macromolecular components of tomato fruit pectin. Arch. Biochem. Biophys. 274: 179–191.
Fishman, M.L., Pfeffer, P.E., Barford, R.A., and Doner, L.W. 1984. Studies of pectin solution properties by high performance size exclusion chromatography. J. Agric. Food Chem. 32: 372–378.
Flory, P.J. 1953. In *Principles of Polymer Chemistry*, p. 611. Cornell University Press, Ithaca, NY.
Hoagland, P.D., Fishman, M.L., Konja, G., and Clauss, E. 1993. Size exclusion chromatography with viscosity detection of complex polysaccharides: component analysis. J. Agric. Food Chem. Accepted for publication.
Jordan, R.C. and Brandt, D.A. 1978. An investigation of pectin and pectic acid in dilute aqueous solution. Biopolym. 17: 2885–2895.
Kato, T., Okamoto, T., Tokuya, T., and Takahashi, A. 1982. Solution properties and chain flexibility of pullulan in aqueous solution. Biopolym. 21: 1623–1633.
Kohn, R. 1975. Ion binding of polyuronates-alginate and pectin. Pure Appl. Chem. 42: 371–397.
Kravtchenko, T.P., Berth, G., Voragen, A.G.J., and Pilnik, W. 1992. Studies on the intermolecular distribution of industrial pectins by means of preparative size exclusion chromatography. Carbohydr. Polym. 18: 253–263.
Mort, A.J., Moerschbacher, B.M., Pierce, M.L., and Maness, N.O. 1991. Problems encountered during the extraction, purification, and chroma-

tography of pectin fragments, and some solutions to them. Carbohydr. Res. 215: 219–227.
Oakenfull, D. and Scott, A. 1984. Hydrophobic interaction in the gelation of high methoxyl pectins. J. Food Sci. 49: 1093–1098.
Press, W.H., Flannery, B.P., Teukolsky, S.A., and Vetterling, W.T. 1988. *Numerical Recipes in C*, p. 547. Cambridge University Press, NY.
Rees, D.A. 1982. Polysaccharide conformation in solutions and gels - recent results on pectins. Carbohydr. Polym. 2: 254–263.
Rees, D.A. and Wight, A.W. 1971. Polysaccharide conformation. Part IV. Model building computations for α-1,4 galacturonan and the kinking function of L-rhamnose residues in pectic substances. J. Chem. Soc. 1971: 1366–1372.
Ms received 12/11/92; revised 2/10/93; accepted 2/27/93.